GREEN SYNTHESIS, CHARACTERIZATION, THERMOGRAVIMETRIC AND ANTIMICROBIAL STUDIES OF Fe(II) COMPLEX WITH LIGANDS CONTAINING AZOMETHINE (-NHN=CH-)

Supported by tetfund TERTIARY EDUCATION TRUST FUND

[1]*IORUNGWA, M.S., [1]ABUH, H., [1]WUANA, R.A., [1]AMUA, Q.M., [1]IORUNGWA, P.D. and [1]DANAT, B. T.
[1]Inorganic/ Physical Chemistry Research Group, Department of Chemistry, Joseph Sarwuan Tarka University Makurdi, 970001-Nigeria
***Correspondence Email:** iorungwa.moses@uam.edu.ng

Received: December 14, 2023 Accepted: March 28, 2024

Abstract: The ligand (**L_1**) of 2, 4-Dinitrophenylhydrazine and 3-Hydroxybenzaldehyde with N-(3-hydroxybenzaldehyde)-p-fluoroaniline ligand (**L_2**) and their Fe(II) complex were prepared using grinding as a solvent-free synthetic method. The new compounds were characterized through melting point, solubility test, molar conductance, UV-Vis and IR spectrophotometry. Thermal stability of the ligands with their Fe(II) complex were studied by thermogravimetric analyses (TGA). Energy of activation (E_a), entropy of activation (ΔS^o), free energy of activation (ΔG), enthalpy of activation (ΔH^o) and collision frequency (Z) were calculated using Coats-Redfern's approximation methods. Surface morphologies of the solid compounds were imaged by scanning electron microscopy (SEM). The particle sizes of the ligands and the metal complex were measured using a particle size analyzer at a diffraction angle of 10.9°. The newly synthesized compounds were screened for their antimicrobial activities. Melting points of the synthesized compounds were in the temperature range of 190 - 194℃ showing that they were fairly stable; solubility in non- polar solvents and molar conductance values (5.6 - 11.20 Ω/cm^{-2}) indicates that the ligands and the complex are non-electrolytic in nature. The IR spectra showed bidentate ligands which coordinated through nitrogen atom of the azomethine and deprotonated oxygen atom of the hydroxyl group. The kinetic parameters revealed that the decomposition reactions of the synthesized compounds followed first order reaction and the activation energy ($kJmol^{-1}$) were 54.05, 25.59 and 25.92 for HL_1, $L_2$and Fe(II) complex respectively. This revealed that HL_1 required extra energy to form activated complex as compared to $L_2$and Fe(II) complex. On the other hand, the collision frequencies were7.06×10^{16}, $4.01 \times 10^{4}$and $7.33 \times 10^{4} s^{-1}$for HL_1, $L_2$and Fe(II) complex signifying extra spaces in HL_1 than$L_2$and Fe(II) complex. Positive values of Gibb's free energy (ΔG) of the synthesized compounds indicates that the decomposition was non-spontaneous, the positive values of ΔH^o showed that enthalpy was the driving force for the decomposition of the synthesized compounds and were exothermic in nature. The antimicrobial studies revealed weak activity against the test bacteria and inactivity against the test fungi by the Schiff base ligands while their metal complexes significantly increased or induced antimicrobial sensitivity against the test microbes. Thus, the Schiff base complex hold promise as powerful and all-around antibacterial agent.

Keywords: Green synthesis, characterization, thermogravimetry, antimicrobial, Fe(II) complex

Introduction

In recent years, biologically important ligands containing azomethines (-NHN=CH-) are subject of interest for many inorganic chemistry researchers. The interest is linked to the pharmacological activity of these organic moieties and their complexes such as analgesics, anti inflammatory, ulcerogenic, antimicrobial and anticancer activities (Kumar *et al*., 2017) which depends on the metal ion, ligands and the structure of the complexes (Salvaganapathy and Raman, 2016). These factors are partly responsible for the ability of these complexes to locate the proper target site of activity and as a consequence their activity (Anitha*et al*., 2011; Salvaganapathy and Raman, 2016). It is known that certain metal ions penetrate through microbe cell walls in the form of complexes, into the cell and deactivate certain enzyme, thus deactivating such microbe (Chohan*et al*., 2020). Furthermore, prior reports have also indicated that efficacies of various antimicrobial agents are often enhanced upon coordination with a suitable metal ion (Kan*et al*., 2013).

Regardless of an enormous amount of antibiotics available for medication, there is still an outbreak of diseases caused by different pathogenic microbes and the development of resistance to antibiotics (Sakr*et al*., 2018). Researchers are as a consequence searching for new antimicrobial agents. Additionally, earlier studies have also revealed that some metal complexes of biologically important compounds such as azomethine exhibited promising antimicrobial activities on chelation (Nomiya*et al*., 2000). Owing to the demand of new metal based antimicrobial agents, metal organic chemistry is becoming an emerging area of research (Terreni*et al*., 2021) due the tormenting predicament of antibiotic resistance and the emergence of multidrug-resistant bacteria strains, which have now become really common in hospitals and risk hindering the global control of infectious diseases caused by microorganism.

This work covers the synthesis, characterization, thermal decomposition and antimicrobial activities of Fe^{2+} complex of azomethine (-NHN=CH-). This is in promotion of the sustained interest in the use of transition metal complexes in the treatment of human diseases against the backdrop of the alarming problem of multi-drugs resistant microorganism world over.

Materials and Methods

Reagents and solvents

Analytical grade reagents purchased from Sigma Aldrich were used without purification. Salicyaldehyde (≥98.5 %), 2, 4-dinitrophenylhydrazine and 4-fluoroaniline were used in the synthesis of the azomethine ligands, iron(II) chloride (99 %) was used to synthesize the metal complex. Others are glacial acetic acid (≥99.5 %), methanol (≥99.9 %),

ethanol (99.8 %), acetone and dimethylsulphoxide (DMSO) (≥99 %) used for solubility test.

Apparatus and Instruments

The apparatus and instruments used were Barnstead electro thermal BI-9100 melting point apparatus with digital thermometer, pH/conductivity series 510 conductivity meters, Perkin Elmer FT-IR spectrophotometer (spectrum BX Model using spectrum version 5.3.1 software), Perkin Elmer spectrophotometer UV-VIS double beam PC scanning spectrophotometer (UVD-2690), using UV-Winlab 2.8.5.04 software version, SB160 heat-stirrer, PW 184 weighing balance, 98-1-B temperature regulating heating mantle, and OV/100/F ovum.

Synthesis of ligand with -NHNCH- (HL_1)

Ligand (HL_1) was obtained by condensing 3-hydroxybenzaldehyde (0.01 mol; 1.22 g) with 2,4-dinitrophenylhydrazine (0.01 mol; 1.98 g) through grinding in a mortar in the presence of catalytic amount of water (4 drops) using pestle for 10 min (Iorungwa *et al*., 2020). The resultant compound was oven dried at70 ºC and yielded 95% of orange colour microcrystalline compound.

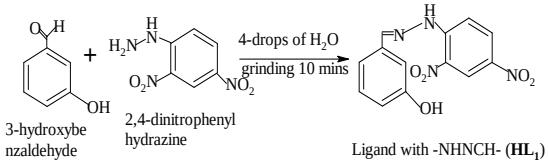

Synthesis of ligand (L_2)

Ligand (L_2) was prepared according to methods described by Ommenya*et al*. (2020) with a few modifications. 4-fluoroaniline (0.3549 g; 0.00319 mol; 0.309 mL) was added to 3-hydroxybenzaldehyde (0.5000 g; 0.00319 mol) in a mortar in the presence of catalytic amount of water (4 drops), was grinded using pestle for 10 min, upon which a thick yellow orange compound was formed instantly. The resulting compound was oven dried at 70 ℃ which formed shiny needle-like yellowish orange crystals.

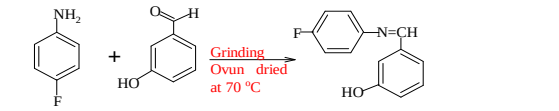

Synthesis of the metal complexcontaining -NHN=CH- as an active group

Fe(II) complex containing -NHN=CH- as an active group was synthesized by mixing the ligands (0.01 mol of HL_1 and L_2) with the metal(II) salt [0.01 mol of Fe(II) salt] as described by Ommenya*et al*. (2020) in a mortar and grounded using pestle for 10 min. The resultant compound was oven dried at 70 ºC and yielded 96 % of colored microcrystalline Fe(II) complex.

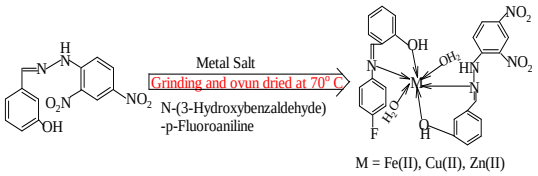

Characterization of the ligands and its complex

Solubility test

Exactly 0.01 g of the prepared ligands and its Fe(II) complex was added to 10 mL portions of distilled water, methanol, ethanol, dimethylsulfoxide, dimethylformamide and acetone in separate test tubes and shaken vigorously. If the entire solute dissolved to give a homogenous mixture after shaking, the sample was considered soluble (S). However, if some dissolved and some were left, the sample was considered to be slightly soluble (SS). If the solute remained as introduced then it means it was insoluble (IS) (Iniama *et al*., 2018).

Melting point determination

A sample of each of the synthesized compounds was filled in separate capillary tubes to a depth of 2 mm and the bottom tapped several times to ensure close packing. The tube was then inserted into the heating block and heated. The temperature at which each of the samples melted was read from the digital screen and recorded (Subin and Aravindakshan, 2017).

Molar conductivity measurement

The conductivity of the ligands alongside the metal complex was carried out at Rolab Research and Diagonistic Laboratory, Ibadan-Nigeria using Accumet AP75 conductivity meter. Water suspension of 1:5 soil was prepared by weighing 10 g air-dry soil (<2 mm) into a bottle and about 50 mL deionised water was added and shaken mechanically at 15 rpm for 1 h to dissolve soluble salts. The conductivity meter was calibrated according to the manufacturer's instructions using the KCl reference solution to obtain the cell constant. The electrical conductivity of the 0.01M KCl was measured and the conductivity values of ligands and their complexes were recorded as indicated on the conductivity meter.

Infrared and electronic spectra studies

The infrared spectra data of the synthesized metal complex was done in KBr discs and displayed on Perkin Elmer 2000 FT-IR spectrophotometer with spectrum version 5.3.1 software. The ultraviolet spectra of the prepared complexes were obtained using acetone as solvent from Perkin Elmer UVD-2690 UV-VIS double beam PC scanning spectrophotometer (UV-Winlab 2.8.5.04) software version.

Thermogravimetric (TGA) study

Thermogravimetric study was carried out as described by Emiola-Sadiq*et al*.(2021). TGA of the synthesized compounds were performed using a TG analyzer (TGA-Q50 series, TA instruments) at standard pressure. About 15 mg of each sample was placed in platinum crucibles and heated linearly at six heating rate, 5 °C/min from ambient room temperature to 650 °C. Nitrogen gas at a flow rate of 60 mL/min was used to purge the system and also provided the inert atmosphere for the experiments. The thermograms revealed changes in the structure and other important properties of ligands and metal complexes. From the TG curves, the thermo-kinetic parameters were obtained at the various decomposition temperatures (200, 250, 300, 350 and 400 °C) using Coat-Redfern approximation by plotting $\log\left(ln\frac{W_c/W_r}{T^2}\right) Vs\left(1/T\right)$which resulted in straight line graphs with slope $\left[-E_a/R\right]$

Antimicrobial studies

The synthesized ligands and theFe(II) complex were tested and evaluated for their antimicrobial activity using the agar diffusion technique (Iorungwa*et al*., 2019). The tested organisms were Gram-negative bacteria (*Escherichia Coli* and*Salmonella typhimurium*), Gram-positive bacteria (*Bacillus subtilis*and*Staphylococcus aureus*). Amoxicillin and nystatin were used as the standard antibacterial and antifugal drugs. The tested bacterial species were grown in Nutrient Agar (NA) medium in petri plates, whereas Sabouraud dextrose agar (SDA) medium was used for fungal species. The media was poured into the sterile petri plates and solidified while the compounds were dissolved in DMF. The inoculum was prepared from the 72 h SDA culture and bacterial species were prepared from a 24 h NA culture. The microbial suspension of each test was evenly spread over the media by sterile cotton swabs. The plates were desiccated and a sterilized cork borer (7 mm in diameter) was used in punching the wells (4 wells) in agar medium. The compounds were thereafter added to the well at different concentration of 25 and 50 mg/mL followed by the diffusion at room temperature for 15 min. The plates were incubated at 37 ℃ for 24 h for bacteria, at 27 ℃ and 72 h for fungi, resulting into the formation of a clear inhibition zone around the well. A meter rule was used in measuring the zone of inhibition. DMF alone was used as a control under the same condition for each organism (El-Barasi*et al*., 2020).

Results and Discussion

The HL_1, L_2 and Fe(II) complex were all coloured (Table 1) . The ligands and the complex were found to melt in the temperature range of 190-194 ^oC showing fairly stable ligands and complex compounds while their conductance values were in the range of 5.6-11.2 $Ohm^{-1}\cdot m^{-1}$ (Table 1) which were below 50 $Ohm^{-1}\cdot m^{-1}$, indicating their non electrolytic nature (Ommenya*et al*., 2020).

Table 1: Physical Properties of Synthesized Ligands with its Complex

Compound	Colour	Melting Point (^oC)	Conductivity ($Ohm^{-1}m^{-1}$)
HL_1	Orange crystals	190.00	5.6
L_2	Orange-yellow crystals	194.00	5.8
Fe(II) complex	Black crystals	194.00	11.20

Table 2: Solubility of Ligands along with Complexes at Room Temperature

Compounds	Distilled Water	Methanol	Ethanol	DMF	Acetone	DMSO	Petroleum ether
HL_1	INS	SS	SS	S	S	S	S
L_2	INS	SS	SS	S	S	S	S
Fe(II) complex	INS	SS	SS	S	S	S	S

Key: S=Soluble SS= slightly soluble INS=Insoluble

Solubility is one of the characteristic properties of ligands and their complexes which mean that solubility is commonly used to describe the ligands and their complexes to indicate their polarity, to help distinguish them from other compounds, and as a guide to application of ligands and their complexes. The ligands and the complex were observed to be insoluble in water but soluble in organic solvents like acetone, dimethylsulphoxide (DMSO), dimethylformaldehyde (DMF) and petroleum ether (Table 2). The insolubility of the ligands with the complex in water indicates the non-polarity which exists in their structures through covalent and coordinate covalent bond; this implies the absence of ionic bond which causes high solubility in water. The insolubility of the complex in water also removes the possibility of counter ions being present in the complex or that the complex is charged. It was noticed that, the solubility of the ligands with the complex improved in organic solvents which could be due to the presence of substituents like -OH,-F and $-NO_2$ at the ortho and para positions of the aromatic ring. The nature of the substituent may help improve the solubility in organic or inorganic media (Das *et al*., 2022).

Table 3: IR Bands (cm^{-1}) of Functional groups for Ligands and its Fe(II) Complex

Compounds	√(N-H)	√(C-OH)	√(C=N)	√(N-N)	√(M-O)	√(M-N)
HL_1	3367	1032	1635	1438		
L_2	3390	1041	1602			
Fe(II) complex	3400	1099	1632	1493	611	499

IR bands at3367 and 1635(HL_1), 3390 and 1602 cm^{-1} (L_2) may be ascribed to the (–NH) and (C =N) respectively (Table 3). The band at 1032 and 1041 cm^{-1} for HL_1 and L_2 are attributed to C-OH.Also, the IR spectrum of the Fe(II) complex, band for (C = N) is seen at 1632 cm^{-1}. This shift in wavenumbersuggests that the (C=N) nitrogen in the

ligand formed a bond with the Fe(II) ion. There is no evidenceof coordination activity from the $–NO_2$ group, since its presence did not shift the location of a band in the metal complex. The new bands in the complexareattributed to the appearance of spectra at 500–510 cm^{-1}and630–650 cm^{-1} to the stretching frequencies of (M–N) and (M–O) bonds respectively (Iorungwa*et al*., 2019; Liu *et al*., 2022).

Table 4: Electronic Spectral Data of the HL_1 and L_2 alongside their Metal Complex

Compounds	λ_{max}(nm)	Assignment	Suggested Structure
HL_1	200.00	$n \rightarrow \pi^*$	
	245.00	$\pi \rightarrow \pi^*$	
	264.00	$\pi \rightarrow \pi^*$	
L_2	205.00	$n \rightarrow \pi^*$	
	213.00	$\pi \rightarrow \pi^*$	
	345.00	$\pi \rightarrow \pi^*$	
Fe(II)	249.00	$n \rightarrow \pi^*$	Tetrahedral
Complex	266.00	$n \rightarrow \pi^*$	
	368.00	$\pi \rightarrow \pi^*$	
	382.00	$\pi \rightarrow \pi^*$	

The Uv-vis spectra of the HL_1,L_2andFe(II) complex from 190 to 900 nmexhibited peaks with notable peaks presented in Table 4. The electronic spectra of HL_1 and L_2 ligands gave three prominent absorption bands at (200, 205) nm, assigned to n→π* of C=N and O-hydroxyl group, respectively. Those at (245, 213) nmare assigned to π→π* of C=N azomethine. The third band was at (264, 345)nm, assigned to π→π* of C=C phenyl. The electronic spectra of Fe(II) complex showed four absorption bands at (249, 266, 368 and 382) nm assigned to n→π* and π→π* transitions, respectively. The observation of these bands suggests an tetrahedral configuration around Fe(II) complex.

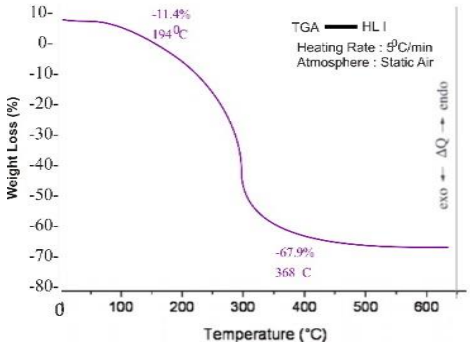

Figure 1a: Thermogram of HL_1

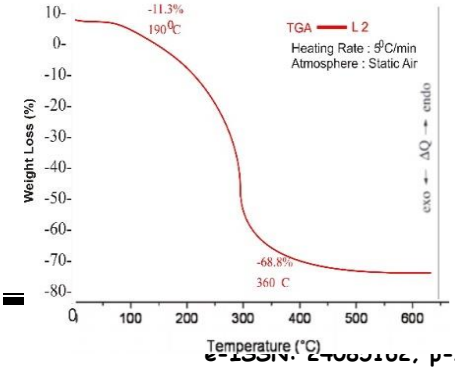

Figure 1b: Thermogram of L_2

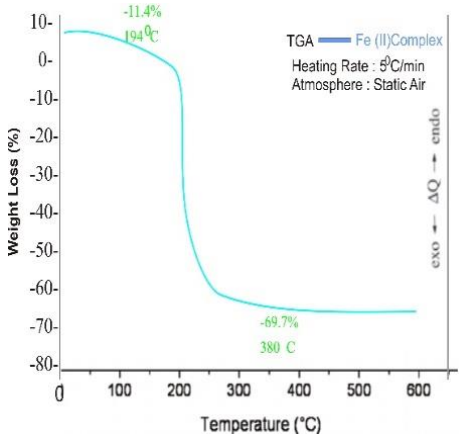

Figures1a-c: TheThemograms of HL_1, L_2 andFe(II) complex

The thermogram of the Fe(II) complex show weight loss from 42 ℃ up to 380 ℃; this indicates the existence of lattice water molecules in it. The Fe(II) complex shows three-steps decomposition process in the range of 42-131 ℃, 131-194 ℃ and 194-380℃.The first step was fairly fast and a total of2.22% weight loss was observed which correspondsto the two molecules of water lattice. In the second step of decomposition starting from 131℃ to 194℃, non chelated part of the ligand was removed which was found to be 11.4 %. The remaining chelated part of the ligand was decomposed in the third stepwhich is 69.7%. The last pyrolysis productlikely to be Fe(II) oxide and some unreactedresidue had an observed mass of 30.3%.

Examining thermogramsof HL_1, L_2 along their Fe(II) complex displayed two decomposition steps whereas the complex showed three decomposition steps in the temperature range 0 ℃ to 650 ℃. This variation in the number of steps of decomposition in HL_1, L_2 and the Fe(II) complex confirmed complexation as suggested by the electronic spectra. It is similarly noticed that the thermograms of the ligands and the complex were curved,this demonstrates that the decomposition reactions followed first order kinetics with the gradient of the curves in the order of $\mathbf{L_2} < \mathbf{HL_1} <$Fe(II) complex. This signifies the speed of the decomposition which could be attributed to the number of electron releasing or withdrawing groups, which increased or lowered the electron density at the reactive centers thereby increasing or decreasing the thermal stability (Doğan*et al*., 2020).

Table 5: Rate of Change of Weight with Temperature obtained from TGA of Ligands and Complex in Nitrogen for Coasts-Redfern Approximation

Compounds	W	W_r	T (K)	$\ln\left(\frac{W_c/W_r}{T^2}\right)$	$\log\left(\ln\frac{W_c/W_r}{T^2}\right)$	$T^{-1}(K^{-1})$
HL_1	6.12	60.04	473.0	-12.221	-1.087	0.00211
	15.01	51.15	523.0	-12.261	-1.089	0.00191
	49.48	16.68	573.0	-11.324	-1.054	0.00175
	61.16	5.00	623.0	-10.287	-1.012	0.00161
	66.16	0.00	673.0	0.000	0.000	0.00149
L_2	13.55	55.25	473.0	-12.099	-1.083	0.00211
	18.55	50.25	523.0	-12.205	-1.087	0.00191
	48.00	20.80	573.0	-11.505	-1.061	0.00175
	63.50	5.30	623.0	-10.306	-1.013	0.00161
	68.80	0.00	673.0	0.000	0.000	0.00149
Fe(II) Complex	2.22	66.17	473.0	-12.285	-1.089	0.00211
	60.05	8.34	523.0	-10.415	-1.018	0.00191
	65.05	3.34	573.0	-9.683	-0.986	0.00175
	66.72	1.67	623.0	-8.989	-0.954	0.00161
	68.39	0.00	673.0	0.000	0.000	0.00149

Key: Wc = weight loss at completion of reaction, W = fraction of weight loss at a particular temperature and w_r = Wc-W

Table 6: Thermal Parameters for Non-isothermal Ligands alongComplexes by TGA in Air using Coats-Redfern Approximation

Compounds	Kinetics Parameters		Thermodynamics Parameters		
	E_a (kj/mol)	Z (s^{-1})	ΔH($kJmol^{-1}$)	ΔG ($kJmol^{-1}$)	ΔS($Jmol^{-1}$)
HL_1	54.05	7.06×10^{16}	50.25	20.19	74.10
L_2	25.59	4.01×10^{4}	21.82	98.20	-160.29
Fe(II) Complex	25.92	7.33×10^{4}	22.07	97.95	-155.57

The thermal parameters of decomposition processes of HL_1, L_2 along its Fe(II) complex, namely, activation energy (E_a), collision frequency (Z), enthalpy (ΔH), entropy (ΔS), and Gibbs free energy change (ΔG), were calculated by the Coats–Redfern method (Fouad*et al*., 2021) (Equation 1)

$$\log\left(\ln\frac{W_c/W_r}{T^2}\right) = \log\left(\frac{ZR}{\phi E_a}\left(1-\frac{2RT}{E_a}\right)\right) - \frac{E_a}{2.303RT} \quad (1)$$

where$W_r = W_c - W$, W_c = mass-loss at the completion of reaction, W = mass-loss up to time 't', Z = collision frequency, R = gas constant = 8.314 $J{\cdot}mol^{-1}{\cdot}K^{-1}$, E_a= energy of activation, T = temperature (K) and ϕ = heating rate = 0.166 s^{-1}.

Since $\frac{1-2RT}{E_a}$ is unity, a plot of $\log\left(ln\frac{W_c/W_r}{T^2}\right) Vs (1/T)$will give a straight line, the slope of which is equal to $E_a/2.303R$ from which E_a andZ can be calculatedusing Equation (2).

$$\text{intercept} = \log\left(\frac{ZR}{\phi E_a}\right) \quad (2)$$

where E_a = activation energy from graph

The kinetic and thermodynamics parameters obtained using Coats-Redfernplot are presented in Table 6. The values of activation energy (kjoules) obtained were 54.05, 25.59 and 25.92 for HL_1, L_2andFe(II) complex respectively. These relative small values of activation energy demonstrates that the rate of decomposition increased with increase in temperature and that the ''apparent'' rate constant of the overall decomposition as defined by Arrhenius behaviour will also increase with temperature increase.This indicate that the decomposition of the ligands and the metal complex had no complex mechanism (Iorungwa*et al*., 2019) and the relatively higher $E_a$for HL_1explains the extra energy needed by HL_1as compared to $L_2$and Fe(II) complex to undergo decomposition. The difference in the values of E_a for the ligands was due to the difference in the nature of chemical bonds.

The collision frequency(Z) can be envisaged as the frequency of properly oriented collisions between reactant particles. The collision frequency values can be used to predict space or volume in the reacting molecules (Vyazovkin, 2021).The values of Z obtained in this study were7.06×10^{16},$4.01 \times 10^{4}$and $7.33 \times 10^{4}$for HL_1, L_2 and Fe(II) complex. These values illustrate that, more space or volume could be present in HL_1than in $L_2$and Fe(II) complex as in Figures 7a-c. The valuesagree with the frequency of collision observed for the ligands and the Fe(II) complex. Theoretically, reducing the value of E_a leads to an increased value of Z while an elevated value of E_a indicates higher stability(Wang *et al*., 2021).

The enthalpy, ΔH, ($KJmol^{-1}$) for HL_1, L_2 and Fe(II) complex were 50.25, 21.82 and 22.07 are positive, indicating that there was decomposition as energy was absorbed during the endothermic reaction. The enthalpy of HL_1 was higher, suggesting that the total energy spent by HL_1 to split into the various components was more than the

energy consumed by L_2, this could be attributed to the extra stability of HL_1, hence, requires greater amount of energy to break the chemical bond present in the ligand (Ohia*et al*., 2013).

The Gibbs free energy (ΔG) values are all positive (Table 6). The positive values show that the process neededenergy to occur, signifying a non-spontaneous process.The entropy value for HL_1 was found to positive 74.10 while L_2 and Fe(II) complex were found to be negative -160.29, -155.57kJoule respectively. The positive value of entropy for HL_1, indicates that the degree of disorderliness of the products formed through dissociation of bonds is higher than that of the reactants whereas the negative values of entropies for L_2 andFe(II) complex, indicates that the degree of disorderliness of the products formed through dissociation of bonds is lower than that of the reactants.

Mmm

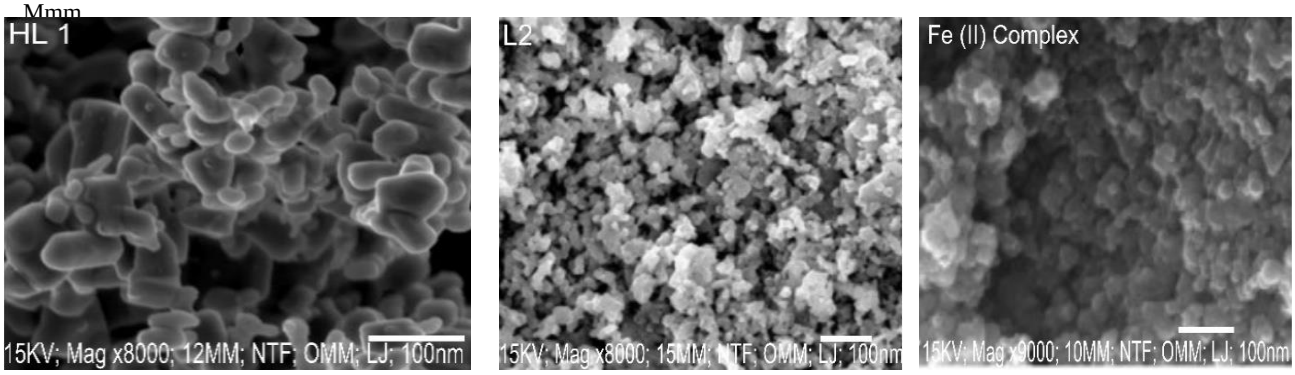

(a) (b) (c)

Figures 2a-c: The SEM Micrographs showing the Morphologies of HL_1, L_2 and its Fe(II) complex

The surface morphology of metal complexes was investigated by scanning electron microscopy. In this study, SEM images were recorded at energy of 20 kV with magnification × 10000 to be used for imaging of the synthesized ligands and metal complex, and carried out morphological studies (texture, pores, and pore's sizes) to determine whether complexation had taken place during grinding. The micrographs (Figures2a-c) show the morphology of the ligands and the metal complex.Comparing these micrographs showed thatcomplexation of ligand with the metal salt had occurred and new product formed which systematically filled the pores in the ligands. The improved physical interconnection of the ligands and metal salt upon complexationresulted in the reduction of the pore's sizes and particle-particle interconnectivity. The cross-sectional view of the micrograph of ligands demonstrates the presence of multiple pores of sizes which are larger than pores observed in the micrograph for the metal complex. This signifies the decrease in porosity upon complexation by filling the pores of the ligand by the metal salts (Zuehlsdorff and Isborn,2017). The SEM micrographs also showed the changesin texture and morphology that accompanythe mixing of ligands and metal salt in the mortar-pestle grinding synthesis of the complex (Figure 2c**)**. The result shows thatthe particle shape and size changedthroughout the complexation process.

Table 7: Diameter of Inhibition Zone of Microbes (nm) of the Synthesized Ligand with its Complex (50 and 100 mg/mL)

Ligands and its metal complex	***S. aureus*** **50 100**	***S. typhi*** **50 100**	***E. coli*** **50 100**	***M. canis*** **50 100**	***C. albican*** **50 100**	***T. rubbrum*** **50 100**
HL_1	9 11	89	8 9	11 11	12 14	-- --
L_2	15 17	10 12	13 14	9 10	12 14	-- --
Fe(II) Complex	19 20	16 17	18 19	13 15	16 16	11 12
Amoxicillin	32 34	28 30	26 28	--	--	--
Nystatin	- -	- -	- -	25 27	29 31	23 25

The synthesized ligands and itsFe(II) complex were tested against bacterial and fungal strains by disc diffusion method. The microorganisms used in the present investigations includedGram-positive*Staphylococcus aureus* and *Staphylococcus typhi* bacterial strains, Gram-negative *Escherichia Coli*.Fungal strains were*Candida albicans*, *Microsporumcanis*and *T. rubrum*. The results were compared with those of the standard drugs (amoxicilin for bacteria and nystatin for fungal). Results of the zones of inhibition measured for ligands (HL_1 and L_2) along itsmetal complexagainst the bacterial and fungal strains are presented inTable 7. Zones of inhibition showed that the ligand (HL_1)was slightly active against*S. aureus* (9, 11 nm), *S. typhi* (8, 9 nm), *E. coli* (8, 9 nm),*M.canis*(11, 11nm) and moderately active against *C. albicans*(12, 14 nm) at a concentration of 100 mg/L but could not inhibit the growth of *Trichophytumrubrum.*However, L_2 was moderately active against *S. aureus*(15, 17 nm), *E. coli* (13,

14 nm) and *C. albican* (12, 14 nm) at a concentration of 100 mg/L but was slightly active against *S. typhi* (10, 12 nm) and *Microsporumcanis* (9, 10) and had no zone of inhibition against *Trichophytumrubrum.*

Fe(II) complex was highly active against *S. aureus*(19,20 mm) and *E. coli*(18, 20 nm) at a concentration of 100 mg/L.However, it was moderately active against *E. coli* only (18 nm) at a concentration of 50 mg/L indicating that, the complex will be more effective at a higher concentration. Also, it was moderately active against *S. typhi* (16, 17 nm), *M. canis* (13, 15 nm) and *C. albican* (16, 16 nm) at both concentrations of 50 and 100 mg/L. Nevertheless, the complex was slightly active against *T. rubrum* (11, 12 nm). The order of activity of Fe(II) complex against the microbes is*T. rubrum*<*M. canis*< *S. typhi* <*C. albican*< *E. coli* < *S. aureus*. In comparison with amoxicilin and nystatin, HL_1 displayed less than 50% inhibition against all test microbes at both concentrations of 50 and 100 mg/mLwhereas L_2displayed 50 % inhibition against *S. aureus* at a concentration of 100 mg/mL and *E. coli* at both concentrations of 50 and 100 mg/mL.This indicates its greater effectiveness against the microbes than HL_1 which could be attributed to some substituents present in L_1.Fe (II) complex displayed more than 50 % inhibition against all the tested microbes as compared with the reference drugs. This enhanced inhibition of the complexcan be explained in terms of the Tweedy's chelation theory. As the metal complex was formed, polarity of the metal ion was reduced to a great extent due to the overlapping of the ligand's orbital and partial sharing of the positive charge of the metal ion with donor groups. Moreover, delocalization of the π-electrons over the whole chelate is increased (Siguh and Chaudhary, 2004).These properties facilitatedthe penetration of the complex across the membrane and DNA of the microbes leading to perturbation of the respiration process of the cell and blocked the synthesis of proteins therebystopping further growth of the organisms. Thus, in extreme cases may lead to the death of the affected microbes (Siguh and Chaudhary, 2004; Aiyelabola *et al.*, 2017).

Conclusion

Ligands HL_1 and L_2 were synthesized with its Fe(II)complex using grinding as a solvent-free synthetic method, the ligands and the complex were characterized and tested for their antimicrobial activities. The solubility result of the ligand and the complex revealed their nonpolarity which was confirmed by molar conductivity results as non-electrolytes. The IR spectra showed that chelation of Fe(II)ion was through the deprotonated hydroxyl group and the azomethine nitrogen thus indicating the bidentate nature of the two ligands. The electronic spectra of the free ligand when compared with that of the complex using various transitions showed a shift from lower to higher frequencies which confirmed the chelation of the two ligands and metal ion. The thermogravimetric analysis results of the ligands revealed that they do not contain even crystals of water while the complex contained crystals of water supporting IR and electronic spectra results. The activation energy obtained from thermal analysis showed that, HL_1 needed additional energy to form activated complex as compare to L_2 andFe(II) complex which was further affirmed by the results of collision frequency. Theresults of Gibb's free energy (ΔG) of the ligands and themetal complex were positive signifying a non-spontaneous process.The positive and negative values of entropy indicate that the degree of disorderliness of the products formed by the dissociationsof the bonds is higher or lower than that of the initial reactants.The antimicrobial studies revealed that the ligands were moderately or slightly active against all the test microbes but not on*T. rubrum*, the metal complex showed significantly enhanced activity against the studied microbial strains in comparison to the free ligands.Their effectiveness as antimicrobial agent was directly proportional to increase in concentrationandtheir activities indicate that the ligands and the metal complex are potential control agents that could be used in an integrated bacteria and fungi management program in comparison with the standard drugs.

References

Anitha, C., Sumathi, S., Tharmaraj, p.andsheela, C.D. (2011). Synthesis, characterization, and biological activities of some transition metal complexes derived from a novel HydrazoneAzo Schiff base ligand. *International journal of inorganic* Chemistry, 9: 1 -12

Aiyelabola, T., Akinkunmi, E., Obuotor, E., Olawuni, I., Isabirye, D. and Jordaan, J. (2017). Synthesis, characterization and biological activities of coordination compounds of 4-hydroxy-3-nitro-2H-chromen-2-one and its aminoethanoic acid and pyrrolidine-2-carboxylic acid mixed ligand complexes. *Bioinorganic Chemistry and Applications*, 1155: 6426747.

Chohan, Z. H., Farooq, M. A., Scozzafava, A. and supurran, C. T. (2020). Antibacterial Schiff bases of oxalyl-Hadrazine; Diamide incorporating pyrrolyl and salicylyl moieties and of their Zinc (II). *Journal of enzyme inhibiton and medicinal chemistry*, 17: 1-7

Das, K. K., Reddy, R. C., Bagoji, I. B., Das, S., Bagali, S.,Mullur, L., Khodnapur, J. P. andBiradar, M. S. (2019). Primary concept of nickel toxicity – an overview. *Journal ofBasic Clinical, Physiological and Pharmacology*, **30**(2): 141–152.

Doğan, S., Tümay, S. O., Balci, C., Yeşilot, S. and Beşli, S. (2020).Synthesis of new cyclotriphosphazene derivatives bearing Schiff bases and their thermal and absorbance properties.*Turkish Journal of Chemistry*, **44**(1): 31 – 47.

Emiola-Sadiq, T., Zhang, L. and Dalai, A. K. (2021).Thermal and kinetic studies on biomass degradation *via*thermogravimetric analysis: A combination of model-fitting and model-free approach. *ACS Omega*, 6: 22233-22247.

Fouad, R., Shaaban, I. A., Ali, T. E., Assiri, M. A. and Shenouda, S. S. (2021). Co(II), Ni(II), Cu(II) and Cd(II)-thiocarbonohydrazonecomplexes: spectroscopic, DFT, thermal, andelectrical conductivity studies. *Royal Society of Chemistry Advances*, 11: 37726-37743.

Iniama, G. E., Iorkpiligh, T. I. &Essien, B. P. (2018). Synthesis, characterization, antibacterial and antifungal activities of Co(II), Ni(II) and Cu(II) Schiff base complexes derived from methionine and salicylaldehyde. *Chemistry Research Journal*, **3**(3): 34-39.

Iorungwa, M. S., Wuana, R. A. &Dafa, S. T. (2019). Synthesis, characterization, kinetics, thermodynamic and antimicrobial studies of Fe(III), Cu(II), Zn(II) N,N'-Bis(2-hydroxy-1,2-diphenylethanone)ethylenediaminecomplexes.*Chemical Methodologies*, **3**: 408-424.

Kan, Y. K., Hsu, Y., Chen, Y.H., Chen, T.C., Weng, J.Y. and Kuo, P.L. (2013).Gemifloxacin, a fluoroquinolone antimicrobial drug, inhibits migration and invasion of human colon cancer cells. *Biomedical Research International*, 13: 1-11

Kumar, S., Pandey, P. K., Sinha, N., Chaudhari, S. &Sharma, S. (2018). Spectroscopic characterisation of metal complexes with tetradentate ligand.*Journal of Physical Science*,**29**(3): 1–11.

Liu S., Elouarzaki, K. and Xu, Z. J. (2022).Electrochemistry in magnetic fields.*Angewandtei*, 61 (27): e202203564.

Nomiya, K., Takahashi, S., Noguchi, R., Nemoto, S., Takayama, T. and Oda, M. (2000). Synthesis and characterization of water-soluble silver(I) complexes with L-Histidine (H2his) and (S)-(-)-2-pyrrolidone-5-carboxylic acid (H2pyrrld) showing a wide spectrum of effective antibacterial and antifungal activities. Crystal structures of chiral helical polymers [Ag(Hhis)]n and {[Ag(Hpyrrld)]2}n in the solid state. *Inorganic Chemistry*, 39: 3301-3311.

Ohia, G. N., Amasiatu, G. I. &Ajagbe, J.O. (2013).*Comprehensive certificate chemistry.2nd edition.*University press Pp. 218-219.

Ommenya, F.K., Nyawade, D.M. and Kinyua, J. (2020). Synthesis, characterization and antibacterial activity of Schiffbase, 4-chloro-2-{(E)-[(4 flurophenyl)imino]methyl}phenol metal (II) complexes. *Journal of Chemistry*, 2020: 1-8.

Sakr, S., Elshafie, H. S., Camele, I. and Sadeek, S. A. (2018). Synthesis, spectroscopic and biological studies of mixed ligand complexes of Gemifloxacin and Glycine with Zn(II), Sn(II) and Ce(III). *Molecules*, 23: 1-17.

Salvaganapathy, M .and Raman, N. (2016). Pharmacological activity of few transition metal complexes: A short Review. *Journal of Chemical Biology and Therapeutic*, 1: 1-10

Subin, K. andAravindakshan, K. (2017). Synthesis, characterization, antimicrobial and antioxidant studies of complexes of Fe(III), Ni(II) and Cu(II) with novel Schiff base ligand (E)-ethyl 3-((2-aminoethyl)imino)butanoate. *Journal of Pharmaceutical, Chemical and Biological Sciences*, **5**(3): 177-186.

Terreni, M., Taccani, M. and Pregnolato, M. (2021). New antibiotics for multidrug- resistant bacterial strains: latest research developments and future perspectives. *Molecules*, **26** (9): 26-71

Wang, Z., He, J., Li, Q., Tang, Y., Wang, J., Pan, Z., Chen, X. and Jiao, X. (2020). First Detection of NDM-5-Positive Salmonella EntericaSerovarTyphimurium Isolated from Retail Pork in China. Microb.*Drug Resistant Larchmot*, 26: 434-437.

Zuehlsdorff, T. J and Isborn, C. M.(2017). Combining the ensemble and Franck-Condon approaches for calculating spectral shapes of molecules in solution. *The Journal of chemical science*, **148**(1): 1-17.